Two numerical solutions for the stochastic collection equation

Martin Simmel

Abstract

Two different methods are used to solve the stochastic collection equation (SCE) numerically. They are called linear discrete method (LDM) and bin shift method (BSM), respectively. Conceptually, both of them are similar to the well-known discrete method (DM) of Kovetz and Olund. For LDM and BSM, their concept is extended to two prognostic moments. Therefore, the "splitting factors" (which are constant in time for DM) become time-dependent for LDM and BSM.

Simulations are shown for the Golovin kernel (for which an analytical solution is available) and the hydrodynamic kernel after Hall. Different bin resolutions and time steps are investigated. As expected, the results become better with increasing bin resolution. LDM and BSM do not show the anomalous dispersion which is a weakness of DM.

Zusammenfassung

Es werden zwei verschiedene Methoden zur numerischen Lösung der "Gleichung für stochastisches Einsammeln" (stochastic collection equation, SCE) vorgestellt. Sie werden als Lineare Diskrete Methode (LDM) bzw. Bin Shift Methode (BSM) bezeichnet. Konzeptuell sind beide der bekannten Diskreten Methode (DM) von Kovetz und Olund ähnlich. Für LDM und BSM wird deren Konzept auf zwei prognostische Momente erweitert. Für LDM und BSM werden die "Aufteil-Faktoren" (die für DM zeitlich konstant sind) dadurch zeitabhängig.

Es werden Simulationsrechnungen für die Koaleszenzfunktion nach Golovin (für die eine analytische Lösung existiert) und die hydrodynamische Koaleszenzfunktion nach Hall gezeigt. Verschiedene Klassenauflösungen und Zeitschritte werden untersucht. Wie erwartet werden die Ergebnisse mit zunehmender Auflösung besser. LDM und BSM zeigen nicht die anomale Dispersion, die eine Schwäche der DM ist.

1 Introduction

For the description of the warm cloud microphysics, the drop growth via collision and coalescence is the prevailing process for drops larger than 20 μm in radius. The coalescence is described by the stochastic collection equation (SCE). The SCE can be solved analytically for various kernels and initial distributions (Golovin 1963, Scott 1968) but not for the hydrodynamic kernel. Numerical solutions of the SCE are given by various authors (Kovetz and Olund 1969, Bleck 1970, Berry and Reinhardt 1974, Hall 1980, Tzivion et al. 1987, 1999, Chen and Lamb 1994, Seesselberg et al. 1996, Bott 1998). If analytical solutions are available, they are used to evaluate the numerical methods.

One can distinguish different approaches. A main difference between the different numerical models is the number of prognostic moments used. Some use only one prognostic moment in each bin (e. g. the drop number concentration or the liquid water content), some use two moments (e. g. both of them). In a one-moment model the average mass

in each bin is fixed, whereas in a two-moment model it can vary within the borders. This is one of the most important advantages of models using two-moment methods.

Two different two-moment approaches are presented which are conceptually and mathematically relatively simple. The loss terms are calculated in the same way for both of the methods. The first one we want to call linear discrete method (LDM) because it is related to the discrete method of KOVETZ AND OLUND (1969) and the gain terms are calculated via a linear approximation of the droplet distribution. The second one is a two step procedure. In a first step, each gain term is assigned to one single bin. In a second step, a certain part of the gain term is shifted to a neighbouring bin. This is a modification of the concept of CHEN AND LAMB (1994). We call it bin shift method (BSM). Both methods are compared to the discrete method (DM) of KOVETZ AND OLUND (1969).

SEESSELBERG ET AL. (1996) follow a totally different concept. Their stochastic approach is based directly on the stochastic process of colliding drops and not on the SCE. Every single collision in a given volume is considered. Although the results are physically almost perfect, the stochastic method cannot be implemented in cloud models because of the extremely long computing times (several hours compared to some minutes for "fast" spectral models based on the SCE). The merit of this method is that it can serve as a benchmark for the simulation results of the faster spectral models, especially when hydrodynamic kernels are used, for which no analytical solutions are available. SEESSELBERG ET AL. (1996) compare the solutions of the stochastic approach to results obtained with the models following BERRY AND REINHARDT (1974) and KOVETZ AND OLUND (1969), slightly modified, respectively. They conclude that the DM of KOVETZ AND OLUND (1969) shows anomalous dispersion despite their own slight modification. Due to the use of two prognostic moments, the two-moment methods presented here do not suffer from this dispersion although the concept followed is very similar.

2 Equation for the moments

The coalescence process is described by the stochastic collection equation (SCE, e. g. PRUPPACHER AND KLETT 1997). It can be written in the form

$$\begin{aligned}\frac{\partial n(x,t)}{\partial t} &= \frac{1}{2}\int_0^x n(x-y,t)n(y,t)K(x-y,y)dy \\ &\quad -n(x,t)\int_0^\infty n(y,t)K(x,y)dy\end{aligned} \tag{1}$$

where $n(x,t)dx$ is the number of drops $\epsilon\,[x, x+dx]$ per unit volume at time t and $K(x,y)$ is the collection kernel.

A single drop of mass x belongs to bin k if

$$x_k \leq x < x_{k+1} \tag{2}$$

with $x_{k+1} = px_k$ and $p = const > 1$. In our simulations we use $p = 2, 2^{1/2}, 2^{1/4}$ and $x_1 = \frac{4}{3}\pi r_1^3 \rho_l$ with $r_1 = 1$ μm and $\rho_l = 1000$ kg m^{-3}. The centre of the interval k is given by $\hat{x}_k = (x_k + x_{k+1})/2$.

The lth moment of the distribution function $n(x,t)$ in bin k is defined as

$$M_k^l = \int_{x_k}^{x_{k+1}} x^l n(x,t)dx \tag{3}$$

After multiplying (1) with x^l and integrating over each bin k, we obtain a set of prognostic equations for the moments in each bin k:

$$\frac{dM_k^l(t)}{dt} = \frac{1}{2}\int_{x_k}^{x_{k+1}}\int_{x_1}^{x} n(x-y,t)n(y,t)K(x-y,y)dy \qquad (4)$$
$$- \sum_{j=1}^{J_{MAX}}\int_{x_k}^{x_{k+1}} x^l n(x,t)dx \int_{x_j}^{x_{j+1}} n(y,t)K(x,y)dy$$

with J_{Max} being the number of bins defined. The first term on the right-handed side describes the gain of bin k due to collisions that result in drops belonging to bin k (gain term). The second term describes the loss of bin k caused by the collision of a drop of bin k with another drop (loss term).

This set of equations has to be solved numerically. For DM, the 0th moment ($M_k^0 = N_k$, drop number density in m^{-3}) in each bin k is the prognostic variable. For LDM and BSM, the 0th moment and the 1st moment ($M_k^1 = M_k$, liquid water content in kg m^{-3}) in each bin k are the prognostic fields.

3 Solution of the equation

To solve the SCE, the gain and loss terms are considered seperately. A simple Euler scheme is used for the time integration.

$$N_k(t+\Delta t) = N_k(t) + \Delta_{gain}N_k(t) - \Delta_{loss}N_k(t) \qquad (5)$$
$$M_k(t+\Delta t) = M_k(t) + \Delta_{gain}M_k(t) - \Delta_{loss}M_k(t) \qquad (6)$$

For DM, only the terms concerning the 0th moment N are considered (eq. (5)).

3.1 The loss term

First, we consider the second term on the right-handed side of (4). It describes the loss of the lth moment of bin k caused by the collision of drops out of the bins k and j, respectively. The interaction of each pair of bins k, j for moment l is

$$WM_{kj}^l(t) = \int_{x_k}^{x_{k+1}} x^l n(x,t)dx \int_{x_j}^{x_{j+1}} n(y,t)K(x,y)dy \qquad (7)$$

The interaction term can be approximated by

$$WM_{kj}^l(t) \approx K_{k,j}\int_{x_k}^{x_{k+1}} x^l n(x,t)dx \int_{x_j}^{x_{j+1}} n(y,t)dy \qquad (8)$$
$$= K_{k,j}M_k^l(t)M_j^0(t) \qquad (9)$$

with $K_{k,j} = K(\hat{x}_k, \hat{x}_j)$. We use the interaction terms for $l = 0, 1$

$$WN_{kj}(t) = K_{k,j}N_k(t)N_j(t) \quad \text{for} \quad l = 0 \qquad (10)$$
$$WM_{kj}(t) = K_{k,j}M_k(t)N_j(t) \quad \text{for} \quad l = 1 \qquad (11)$$

Therefore, the loss terms for bin k are

$$\Delta_{loss}N_k(t) = \sum_{j=1}^{J_{Max}} WN_{kj}(t)\Delta t \qquad (12)$$

$$\Delta_{loss}M_k(t) = \sum_{j=1}^{J_{Max}} WM_{kj}(t)\Delta t \qquad (13)$$

For DM, only (10) and (12) are used.

3.2 The gain term

Determining the gain term is mathematically more demanding than calculating the loss term because of the double integral in the SCE. By introducing the "splitting factors" G_{kij} and H_{kij}, the gain terms for bin k can be written as

$$\Delta_{gain}N_k(t) = \sum_{i=2}^{J_{Max}}\sum_{j=1}^{i-1} G_{kij}WN_{ij}(t)\Delta t + \frac{1}{2}\sum_{i=1}^{J_{Max}} G_{kii}WN_{ii}(t)\Delta t \tag{14}$$

$$\Delta_{gain}M_k(t) = \sum_{i=2}^{J_{Max}}\sum_{j=1}^{i-1} H_{kij}(WM_{ij}(t) + WM_{ji}(t))\Delta t + \sum_{i=1}^{J_{Max}} H_{kii}WM_{ii}(t)\Delta t \tag{15}$$

The first term on the right-handed side of each equation describes the gain due to collisions of drops $i > j$, the second term describes the gain due to collisions of equal-sized drops i. The problem reduces to finding the appropriate "splitting factors" G_{kij} and H_{kij} for every possible collision. In most of the cases, $G_{kij} = H_{kij} = 0$. $G_{kij} \neq 0$ ($H_{kij} \neq 0$) means that a collision of two drops out of the bins i and j, respectively, contributes to bin k in terms of N (M).

In the following, we describe three different ways of numerically determining G_{kij} and H_{kij}. First, we review the discrete method of KOVETZ AND OLUND (1969). Due to the so-called anomalous dispersion of the discrete method, a slight modification was proposed by SEESSELBERG ET AL. (1996). The discrete method is a one-moment scheme with a fixed average mass in each bin. Therefore, we only have to consider (14) and to determine G_{kij}.

Then, we explain two conceptually similar methods. Like DM, both of our solutions are mathematically relatively simple. The solution for the gain term of (4) is derived by posing the question to which bin(s) the loss terms of other bins contribute. This question can be answered by looking at the sum of the masses of the two drops colliding. In contrast to DM, the splitting factors are time-dependent for LDM and BSM. This leads to a more realistic description of the coalescence process.

3.2.1 Discrete method

Two drops out of the bins k and j collide and form a new drop of mass x_n with

$$x_k + x_j \leq x_n \leq x_{k+1} + x_{j+1} \tag{16}$$

For $k \neq j$ we can find bins i and $i+1$ with

$$x_i \leq x_k + x_j \leq x_{i+1} \leq x_{k+1} + x_{j+1} \leq x_{i+2} \tag{17}$$

The contributions resulting from the collisions of drops out of the bins k and j have to be split up into the bins i and $i+1$. Number conservation yields

$$G_{ikj} + G_{i+1kj} = 1 \tag{18}$$

and mass conservation

$$G_{ikj}\hat{x}_i + G_{i+1kj}\hat{x}_{i+1} = \hat{x}_k + \hat{x}_j \tag{19}$$

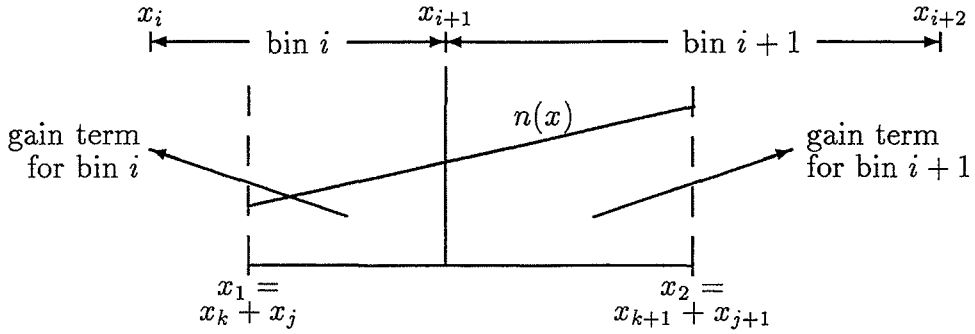

Figure 1: *The linear approximation to the distribution of the loss terms of bins k, j because of their interaction with each other is used to calculate the part of the source terms for the bins i and $i+1$ caused by this interaction.*

For $k = j$, one single bin i is found with

$$x_i = 2x_k \text{ and } x_{i+1} = 2x_{k+1} \tag{20}$$

because of the choice of p. $G_{ikj} = 1$ in this case.

Due to the anomalous dispersion of the discrete method, SEESSELBERG ET AL. (1996) replaced (18) by the following condition

$$G_{ikj}\hat{x}_i^2 + G_{i+1kj}\hat{x}_{i+1}^2 = (\hat{x}_k + \hat{x}_j)^2 \tag{21}$$

This modification is used in the simulations presented here. For $k \neq j$, this leads to

$$G_{ikj} = \begin{cases} \left(\frac{\hat{x}_k+\hat{x}_j}{\hat{x}_i}\right)\left(\frac{\hat{x}_{i+1}-(\hat{x}_k+\hat{x}_j)}{\hat{x}_{i+1}-\hat{x}_i}\right) & \text{if } \hat{x}_i \leq \hat{x}_k + \hat{x}_j < \hat{x}_{i+1} \\ \left(\frac{\hat{x}_k+\hat{x}_j}{\hat{x}_i}\right)\left(\frac{\hat{x}_k+\hat{x}_j-\hat{x}_i}{\hat{x}_i-\hat{x}_{i-1}}\right) & \text{if } \hat{x}_{i-1} \leq \hat{x}_k + \hat{x}_j < \hat{x}_i \\ 0 & \text{otherwise} \end{cases} \tag{22}$$

3.2.2 Linear discrete method

The "gain bins" i and $i+1$ for a collision of two drops out of the bins k and j are determined in the same way as for DM. For $k = j$, $G_{ikj} = H_{ikj} = 1$ if (20) is true and $G_{ikj} = H_{ikj} = 0$ otherwise. The splitting of N and M between the bins i and $i+1$ for $k > j$ is calculated via the linear approximation described in appendix A. It is applied with

$$x_1 = x_k + x_j \tag{23}$$
$$x_2 = x_{k+1} + x_{j+1} \tag{24}$$
$$N = WN_{kj}\Delta t \tag{25}$$
$$M = (WM_{kj} + WM_{jk})\Delta t \tag{26}$$

Two colliding drops form *one* new larger drop. Therefore, in (25) *one* of the terms WN_{kj} and WN_{jk} is chosen ($WN_{kj} = WN_{jk}$). The mass of the new drop is the sum of the two smaller drops, therefore we have to consider *both* terms WM_{kj} and WM_{jk} in (26) (in general $WM_{kj} \neq WM_{jk}$).

After determining the parameters of the linear approximation, the gain terms are calculated analytically by integrating the linear approximation of the distribution function

from x_1 to x_{i+1} (gain terms for bin i: $\Delta_{kj}N_i$, $\Delta_{kj}M_i$) and from x_{i+1} to x_2 (gain terms for bin $i+1$: $\Delta_{kj}N_{i+1}$, $\Delta_{kj}M_{i+1}$), respectively, for the 0th and the 1st moment (see figure 1). Due to the time dependence of the linear aproximation, G_{ikj} and H_{ikj} are time-dependent as well.

$$G_{ikj} = \Delta_{kj}N_i/(WN_{kj}\Delta t), \quad H_{ikj} = \Delta_{kj}M_i/((WM_{kj} + WM_{jk})\Delta t) \tag{27}$$

$$G_{i+1kj} = \Delta_{kj}N_{i+1}/(WN_{kj}\Delta t), \quad H_{i+1kj} = \Delta_{kj}M_{i+1}/((WM_{kj} + WM_{jk})\Delta t) \tag{28}$$

3.2.3 Bin shift method

In contrast to the methods described above, the interaction terms of the bins k, j are assigned only to one single bin i. This bin i is found by checking if the sum of the centres of the bins k, j belongs to bin i.

$$x_i \leq \hat{x}_k + \hat{x}_j \leq x_{i+1} \tag{29}$$

Then the terms defined in (25) and (26) are considered as gain terms for bin i. In other words, we set $G_{ikj} = H_{ikj} = 1$ if (29) is true and $G_{ikj} = H_{ikj} = 0$ otherwise.

In a second step, after (5) and (6) are evaluated, the bin shift (CHEN AND LAMB 1994) is applied (see appendix B).

4 Results and discussion

We present simulation results for the numerical methods described in the previous section. We did simulations for different resolutions ($p = 2$ and $p = 2^{1/4}$) for the Golovin kernel (GOLOVIN 1963) and for the hydrodynamic kernel after HALL (1980). As initial distribution we use the same exponential function as TZIVION ET AL. (1987, 1999).

$$n(x) = 4\frac{N_0 x}{x_0^2}\exp[-2x/x_0] \tag{30}$$

with $N_0 = 3 \cdot 10^8$ m^{-3} and $x_0 = 3.33 \cdot 10^{-12}$ kg for the simulations with the Golovin kernel and $N_0 = 10^8$ m^{-3} and $x_0 = 10^{-11}$ kg for the Hall kernel. This corresponds to a liquid water content of 1 g m^{-3} in both cases.

For all runs the water mass is conserved (except numerical inaccuracies).

4.1 Golovin kernel

Using the Golovin kernel, the SCE can be solved analytically for various initial distributions (GOLOVIN 1963, SCOTT 1968). The Golovin or "sum of mass" kernel is given as

$$K(x, y) = b(x + y) \tag{31}$$

with $b = 1.5$ m^3 s^{-1} kg^{-1} and x, y the mass of the colliding drops. Out of all kernels for which an analytical solution of the SCE is known, the Golovin kernel is closest to the hydrodynamical kernel and therefore is a good test for the numerical method used.

Figure 2 shows the mass distribution after an integration time of 15, 30, 45, and 60 minutes for DM, LDM, and BSM compared to the analytical solution (GOLOVIN 1963) for $p = 2$ (left) and for $p = 2^{1/4}$ (right). For $p = 2$, one can clearly see the anomalous dispersion of DM, which is not shown by LDM and BSM. LDM seems to overestimate the coalescence growth, whereas BSM seems to underestimate this growth. LDM is closer

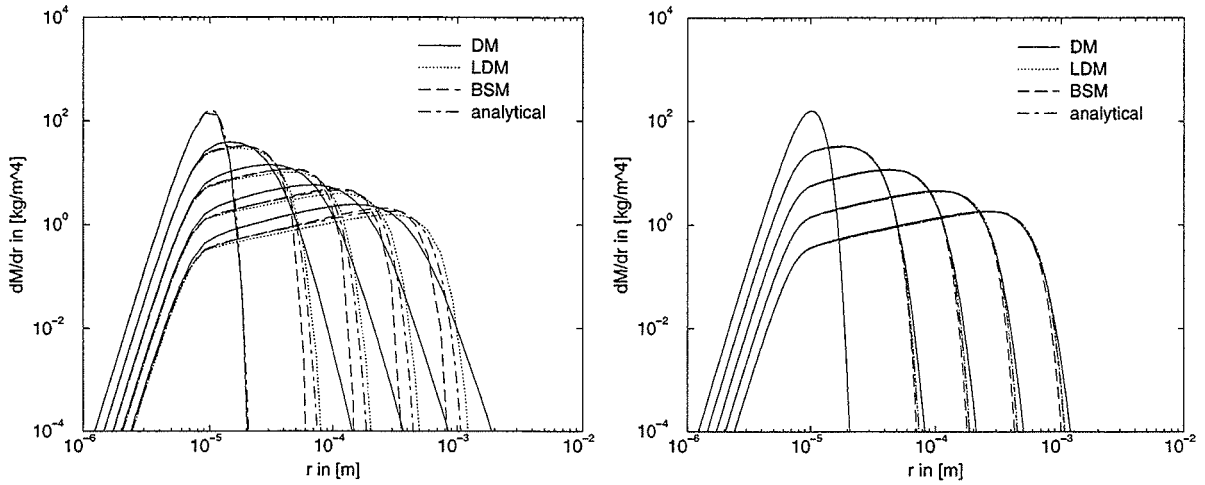

Figure 2: *Mass distribution for the Golovin kernel using DM, LDM, and BSM with $p = 2$ (left) and $p = 2^{1/4}$ (right) compared to the analytical solution. Results are shown after 0 (initial distribution), 15, 30, 45, and 60 min., respectively, time step was 1 s.*

to the analytical solution than BSM. With increasing resolution ($p = 2^{1/4}$, fig. 2, right), the analytic solution is approximated almost perfectly by all methods and the different solutions show nearly the same results. The time step used was 1 s.

Figure 3 shows the simulation results for LDM (left) and BSM (right) using different time steps (1 s, 3 s, and 10 s). The behaviour is the same for both of the schemes: The growth for the 10 s time increment is slightly retarded compared to the other two (1 s and 3 s), which are almost identical ($p = 2^{1/4}$). This means that time steps up to 10 s can be used in the models with only small errors.

The results shown here are comparable to those presented by other authors using different numerical methods (e. g. TZIVION ET AL. 1987, 1999, SEESSELBERG ET AL. 1996, BOTT 1998, and others).

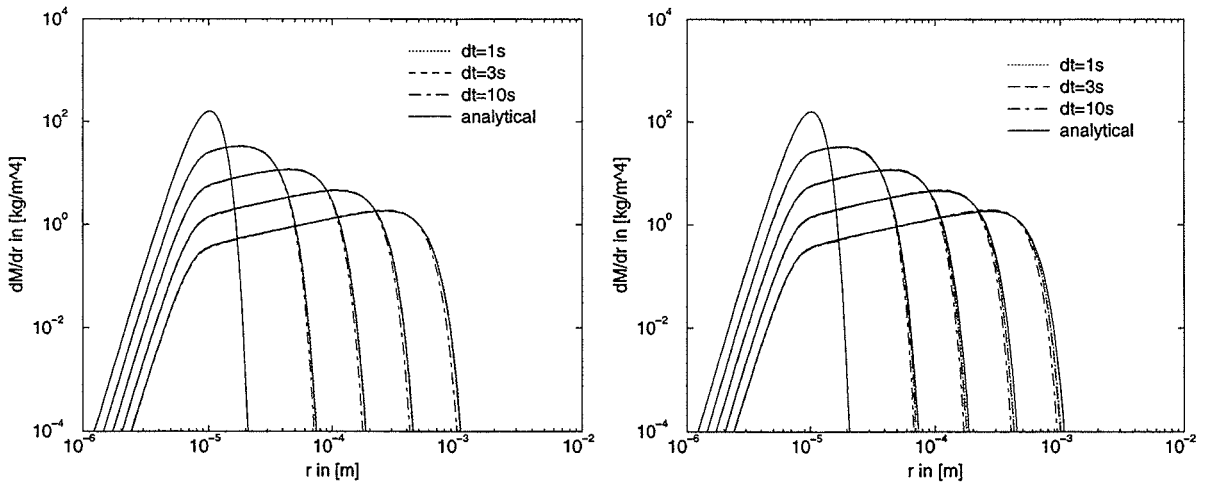

Figure 3: *Mass distribution for the Golovin kernel using LDM (left) and BSM (right) with different time steps $dt = 1$ s, $dt = 3$ s, and $dt = 10$ s compared to the analytical solution. Resolution was $p = 2^{1/4}$. Results are shown after 0 (initial distribution), 15, 30, 45, and 60 min., respectively.*

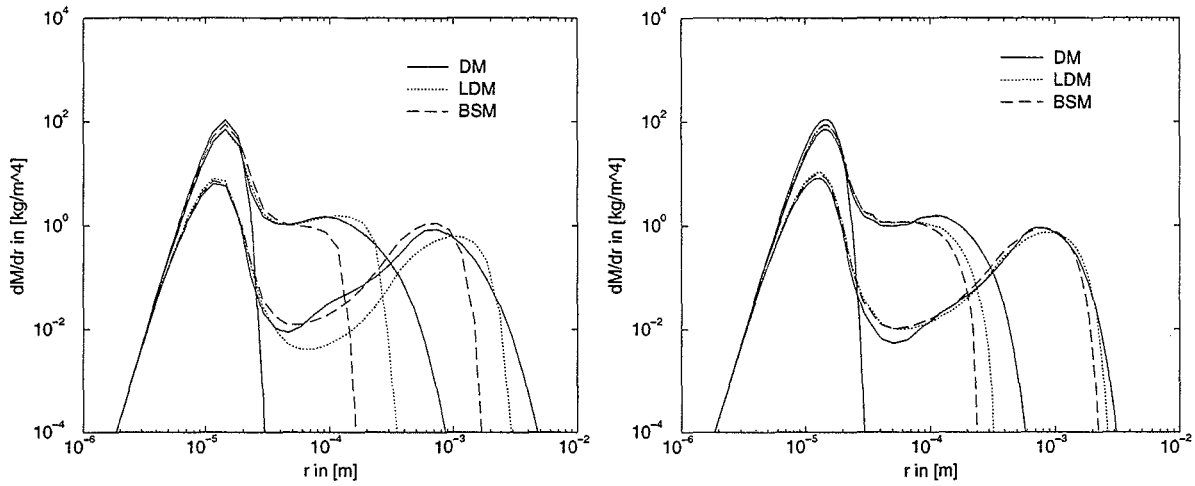

Figure 4: *Mass distribution for the Hall kernel using DM, LDM, and BSM with $p = 2$ (left) and $p = 2^{1/4}$ (right). Results are shown after 0 (initial distribution), 20, and 40 min., respectively, time step was 1 s.*

4.2 Hydrodynamic kernel

The hydrodynamic kernel is defined as

$$K(x,y) = \pi(r_x + r_y)^2 E_{coll}(x,y) E_{coal}(x,y) |v_x - v_y| \tag{32}$$

with the terminal fall velocity v and the collection efficiency $E(x,y)$, which is given as

$$E(x,y) = E_{coll}(x,y) E_{coal}(x,y) \tag{33}$$

with collision efficiency $E_{coll}(x,y)$ and the coalescence efficiency $E_{coal}(x,y)$. Different datasets and theoretical investigations are used in spectral simulations (DAVIS 1972, JONAS 1972, LIN AND LEE 1975, HALL 1980). For our simulations we choose one of the most used datasets for the collision efficiency which is the one of HALL (1980). The coalescence efficiency is assumed to be unity and the terminal velocity is taken from BEARD (1976).

Figure 4 shows the results for DM, LDM, and BSM for $p = 2$ (left) and $p = 2^{1/4}$ (right) after 20 and 40 min. simulation time, respectively. For $p = 2$, the solutions obtained using the three methods, differ very much. Again, DM shows a strong dispersion. LDM overestimates the growth and BSM underestimates the growth. For higher resolutions ($p = 2^{1/4}$), solutions for the three methods approach each other. The real solution should be somewhere in between LDM and BSM and closer to LDM. This is due to the fact that the LDM solutions for $p = 2$ and $p = 2^{1/4}$, respectively, differ not as much as the BSM solutions for the same resolutions (compare fig. 4 left and right).

Figure 5 shows the results for LDM (left) and BSM (right) using different time steps (1 s, 3 s, and 10 s with $p = 2^{1/4}$). Like for the Golovin kernel, the use of a larger time step leads to a slight underestimation of the growth. The hydrodynamic kernel seems to be a bit more sensitive to the variation of the time step than the Golovin kernel.

Generally, it can be said that the errors for the simulations using the hydrodynamic kernel are only slightly larger than those for the ones using the Golovin kernel. This supports the assumption that if a model shows good results for the Golovin kernel it will give good results for the hydrodynamic kernel as well. General tendencies are the same for different kernels: Strong dispersion for DM (especially for low resolutions), slight overestimation for LDM and underestimation for BSM. The weakness of each method is

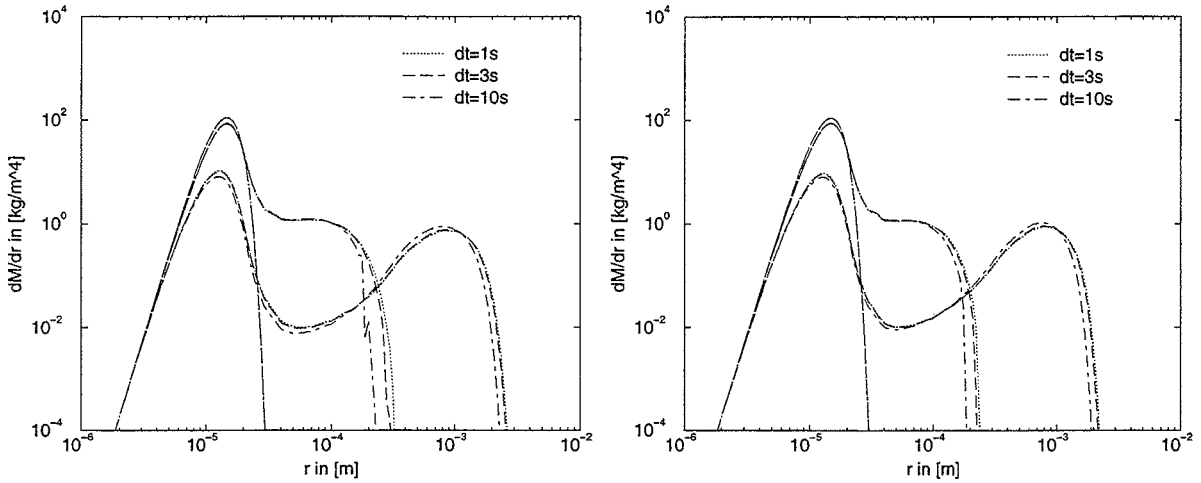

Figure 5: *Mass distribution for the Hall kernel using LDM (left) and BSM (right) with different time steps* $dt = 1$ *s,* $dt = 3$ *s, and* $dt = 10$ *s. Resolution was* $p = 2^{1/4}$*. Results are shown after 0 (initial distribution), 20, and 40 min., respectively.*

seen best when using a low resolution. Solutions using high resolutions and small time steps are good benchmarks if there are no systematic errors included. LDM seems to give the best results for both kernels as well as for all bin resolutions used.

4.3 Computation times

Table 1 shows the computation times for the runs performed. One expects that DM needs less time than LDM and BSM due to the fact that DM is a one-moment method. This is true only for small resolutions. The time consumption of DM and LDM grows roughly proportional to the square of the bin number J_{Max} when the resolution increases. This corresponds to the number of interaction terms. BSM needs less time than LDM (especially for high resolutions) because each time step the linear approximation has to be applied only once per *bin* (which is J_{Max}), whereas for LDM it has to be applied once per *interaction term* (which is J^2_{Max}). Therefore, time consumption of BSM does not grow as strong as for DM and LDM with increasing resolution and for high resolutions, DM even needs more time than BSM.

Generally, empty bins are not taken into account to save computation time. Therefore, underestimation of the growth saves computation time (BSM) whereas overestimation (LDM) or dispersion (DM) lead to longer computation times. These effects should be small.

	Golovin kernel		Hall kernel	
	$p = 2$	$p = 2^{1/4}$	$p = 2$	$p = 2^{1/4}$
DM	3.86 s	53.70 s	2.50 s	36.50 s
LDM	6.23 s	97.61 s	3.30 s	51.91 s
BSM	5.80 s	65.91 s	3.08 s	27.27 s

Table 1: *Run times of the runs performed on an IBM RS6000. For the Golovin kernel the integration time was 60 min., for the Hall kernel 40 min.*

5 Summary

Two spectral models for a numerical solution of the SCE were presented. They follow a similar concept as the discrete method of KOVETZ AND OLUND (1969).

For the Golovin and the Hall kernel, simulations with different resolutions and timesteps were carried out. For the Golovin kernel, the results were compared to the analytical solution. For the Hall kernel, no analytical solution is available. Therefore, the results of different methods, time steps and bin resolutions only can be compared to each other. Generally, the errors for the Hall kernel are somewhat larger than for the Golovin kernel when using the same model parameters. For both kernels, DM shows an anomalous dispersion, especially for low resolutions. Despite following the same concept as DM, LDM and BSM do not show dispersion. This is due to the fact that two prognostic moments are used and therefore, the splitting factors are time-dependent. For growing resolution, the numerical solutions approach the real solution.

LDM seems to give the best results (for both kernels and all resolutions), but needs the most computing time as well. The one-moment method DM is faster than the two-moment method BSM only for low resolutions; for high resolutions BSM is faster.

Appendix

A Linear approximation

Using the first two moments $N = N_k$ and $M = M_k$, one can calculate a linear approximation of the distribution function for each bin k. This was done by CHEN AND LAMB (1994). The linear approximation is valid in for an interval with the lower border $x_1 = x_k$, the upper border $x_2 = x_{k+1}$, and the centre $x_0 = \hat{x}_k$, and is defined as

$$n(x) = n_0 + a(x - x_0) \tag{34}$$

Using the definition of the moments (Eq. (3) for $l = 0, 1$) and substituting $n(x)$ by (34) we obtain

$$N = \int_{x_1}^{x_2} (n_0 + a(x - x_0))\, dx \tag{35}$$

$$M = \int_{x_1}^{x_2} x(n_0 + a(x - x_0))\, dx \tag{36}$$

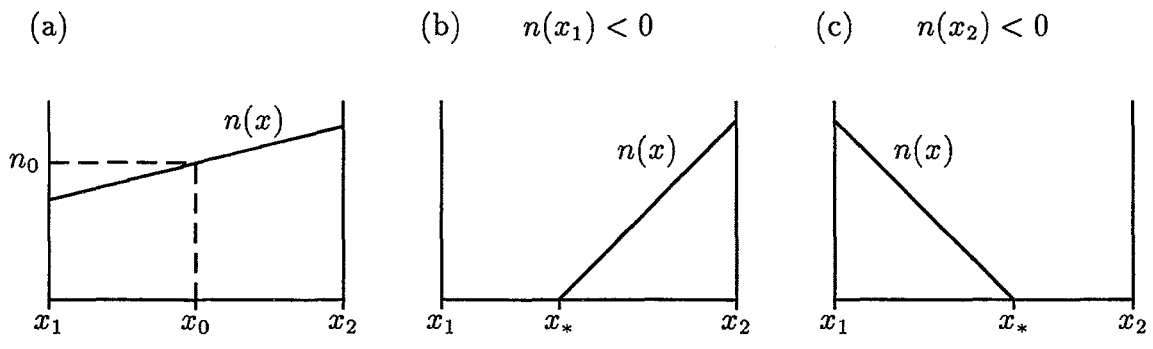

Figure 6: *Linear approximation of the drop distribution function: (a) standard (eq. (34)), (b) alternative formulation (eq. (39)) for* $n(x_1) < 0$ *and (c)* $n(x_2) < 0$*, respectively.*

After some transformations we get the two parameters

$$n_0 = \frac{N}{x_2 - x_1} \tag{37}$$

$$a = \frac{12(M - x_0 N)}{(x_2 - x_1)^3} \tag{38}$$

Depending on N and M, $n(x_1)$ or $n(x_2)$ may become negative for the values of n_0 and a calculated above. This is unphysically, the positiveness of the distribution over the interval has to be guaranteed. Therefore, if $n(x_1) < 0$ or $n(x_2) < 0$, the linear approximation is defined alternatively

$$n_*(x) = a_*(x - x_*) \tag{39}$$

Then the new parameters n_* and x_* are determined using

$$N = \int_{x_*}^{x_2} a_*(x - x_*)\, dx, \quad M = \int_{x_*}^{x_2} x a_*(x - x_*)\, dx \quad \text{for } n(x_1) < 0 \tag{40}$$

$$N = \int_{x_1}^{x_*} a_*(x - x_*)\, dx, \quad M = \int_{x_1}^{x_*} x a_*(x - x_*)\, dx \quad \text{for } n(x_2) < 0 \tag{41}$$

which gives

$$x_* = \frac{3M}{N} - 2x_2, \quad a_* = \frac{2N}{(x_2 - x_*)^2}, \quad \text{for } n(x_1) < 0 \tag{42}$$

$$x_* = \frac{3M}{N} - 2x_1, \quad a_* = \frac{-2N}{(x_1 - x_*)^2}, \quad \text{for } n(x_2) < 0 \tag{43}$$

The three possible linear approximations are shown in figure 6.

B The bin shift

Bin shift means that the whole bin k is shifted by a certain value Δx due to the microphysical process. This has the consequence that if $\Delta x > 0$ ($\Delta x < 0$) the largest (smallest) drops of the bin are moved to the next larger (smaller) bin. CHEN AND LAMB (1994) describe two different ways of determining Δx and the new borders of the shifted bin. We assume that the whole bin is shifted by Δx which is determined as the difference between the average drop mass after the coalescence process and before, respectively.

$$\Delta x = \bar{x}_k' - \bar{x}_k = \frac{M_k(t + \Delta t)}{N_k(t + \Delta t)} - \frac{M_k(t)}{N_k(t)} \tag{44}$$

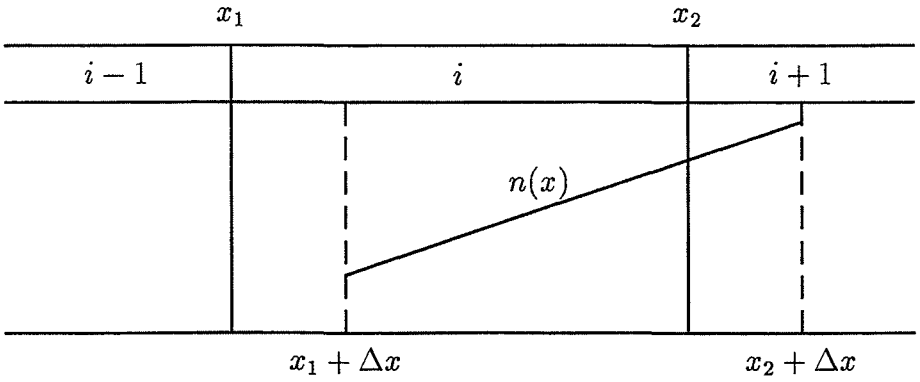

Figure 7: *Transfer of drops from bin i to bin $i+1$ using the bin shift.*

Therefore, the shifted borders are

$$x_1 = x_k + \Delta x \text{ and } x_2 = x_{k+1} + \Delta x \tag{45}$$

The linear approximation for this new distribution (with $x_1, x_2, N_k(t + \Delta t), M_k(t + \Delta t)$) is calculated as described in appendix A. The contributions for the respective bins are calculated by integrating over the intervals (see figure 7). So a remapping of the shifted intervals to the fixed bins is carried out.

Acknowledgements

This work was supported by the Deutsche Forschungsgemeinschaft (DFG) under contract TE 51/11-1.

References

BEARD, K. V., 1976. Terminal velocity and shape of cloud and precipitation drops aloft. *Journal of the Atmospheric Sciences*, **33**, 851–864.

BERRY, E. X. AND R. L. REINHARDT, 1974. An analysis of cloud drop growth by collection. Part I: Double distributions. *Journal of the Atmospheric Sciences*, **31**, 1814–1824.

BLECK, R., 1970. A fast, approximative method for integrating the stochastic coalescence equation. *Journal of Geophysical Research*, **75**, 5165–5171.

BOTT, A., 1998. A flux method for the numerical solution of the stochastic collection equation. *Journal of the Atmospheric Sciences*, **55**, 2284–2293.

CHEN, J.-P. AND D. LAMB, 1994. Simulation of cloud microphysical and chemical processes using a multicomponent framework. Part I: Description of the microphysical model. *Journal of the Atmospheric Sciences*, **51**, 2613–2630.

DAVIS, M. H., 1972. Collisions of small cloud droplets: Gas kinetic effects. *Journal of the Atmospheric Sciences*, **29**, 911–915.

GOLOVIN, A. M., 1963. The solution of the coagulation equation for cloud droplets in a rising air current. *Bull. Acad. Sci. USSR Geophys. Ser.*, **5**, 783–791.

HALL, W. D., 1980. A detailed microphysical model within a two-dimensional dynamic framework: Model description and preliminary results. *Journal of the Atmospheric Sciences*, **37**, 2486–2507.

JONAS, P. R., 1972. The collision efficiency of small drops. *Quarterly Journal of the Royal Meteorological Society*, **98**, 681–683.

KOVETZ, A. AND B. OLUND, 1969. The effect of coalescence and condensation on rain formation in a cloud of finite vertical extent. *Journal of the Atmospheric Sciences*, **26**, 1060–1065.

LIN, C. L. AND S. C. LEE, 1975. Collision efficiency of water drops in the atmosphere. *Journal of the Atmospheric Sciences*, **32**, 1412–1418.

PRUPPACHER, H. R. AND J. D. KLETT, 1997. *Microphysics of clouds and precipitation.* Kluwer Academic Publisher.

SCOTT, W. T., 1968. Analytic studies of cloud droplet coalescence. *Journal of the Atmospheric Sciences*, **25**, 54–65.

SEESSELBERG, M., T. TRAUTMANN, AND M. THORN, 1996. Stochastic simulations as a bench-mark for mathematical methods solving the coalescence equation. *Atmospheric Research*, **40**, 33–48.

TZIVION, S., G. FEINGOLD, AND Z. LEVIN, 1987. An efficient numerical solution to the stochastic collection equation. *Journal of the Atmospheric Sciences*, **41**, 1648–1661.

TZIVION, S., T. G. REISIN, AND Z. LEVIN, 1999. A numerical solution of the kinetic collection equation using high spectral grid resolution: A proposed reference. *Journal of Computational Physics*, **148**, 527–544.

Address of the author:

Martin Simmel
Institut für Meteorologie
Universität Leipzig
Stephanstr. 3
04103 Leipzig
smartie@dynamics.meteo.uni-leipzig.de